Article:
Hall, X.J., Palmese, A., O'Connor, B. et al. (2026) AT2025ulz and S250818k: Leveraging DESI spectroscopy in the hunt for a kilonova associated with a subsolar-mass gravitational-wave candidate. The Astrophysical Journal Letters, 1001 (1). L20. ISSN: 2041-8205

https://doi.org/10.3847/2041-8213/ae4338

The Astrophysical Journal Letters, 1001:L20 (15pp), 2026 April 10 https://doi.org/10.3847/2041-8213/ae4338

AT2025ulz and S250818k: Leveraging DESI Spectroscopy in the Hunt for a Kilonova Associated with a Subsolar-mass Gravitational-wave Candidate

Xander J. Hall[1], Antonella Palmese[1], Brendan O'Connor[1,31], Daniel Gruen[2,3], Malte Busmann[2], Julius Gassert[1,2], Lei Hu[1], Ignacio Magaña Hernandez[1], Jessica Nicole Aguilar[4], Ariel Amsellem[1], Steven Ahlen[5], John Banovetz[4], Segev BenZvi[6], Davide Bianchi[7,8], David Brooks[9], Francisco Javier Castander[10,11], Todd Claybaugh[4], Andrei Cuceu[4], Arjun Dey[12], Peter Doel[9], Jennifer Fabà-Moreno[2], Simone Ferraro[4,13], Andreu Font-Ribera[14], Jaime E. Forero-Romero[15], Gaston Gutierrez[16], Laurent Le Guillou[17], Dick Joyce[12], Theodore Kisner[4], Anthony Kremin[4], Ofer Lahav[9], Claire Lamman[18], Martin Landriau[4], Michael Levi[4], Axel de la Macorra[19], Marc Manera[14,20], Aaron Meisner[12], Ramon Miquel[14,21], John Moustakas[22], Seshadri Nadathur[23], Francisco Prada[24], Ignasi Pérez-Ràfols[25], Graziano Rossi[26], Eusebio Sanchez[27], David Schlegel[4], Michael Schubnell[28], David Sprayberry[12], Gregory Tarlé[29], Benjamin Alan Weaver[12], Rongpu Zhou[4], Hu Zou[30] The Dark Energy Spectroscopic Instrument Collaboration

[1] McWilliams Center for Cosmology and Astrophysics, Department of Physics, Carnegie Mellon University, 5000 Forbes Ave., Pittsburgh, PA 15213, USA; xhall@cmu.edu
[2] University Observatory, Faculty of Physics, Ludwig-Maximilians-Universität München, Scheinerstr. 1, 81679 Munich, Germany
[3] Excellence Cluster ORIGINS, Boltzmannstr. 2, 85748 Garching, Germany
[4] Lawrence Berkeley National Laboratory, 1 Cyclotron Rd., Berkeley, CA 94720, USA
[5] Department of Physics, Boston University, 590 Commonwealth Ave., Boston, MA 02215, USA
[6] Department of Physics & Astronomy, University of Rochester, 206 Bausch and Lomb Hall, P.O. Box 270171, Rochester, NY 14627-0171, USA
[7] Dipartimento di Fisica "Aldo Pontremoli," Università degli Studi di Milano, Via Celoria 16, I-20133 Milano, Italy
[8] INAF-Osservatorio Astronomico di Brera, Via Brera 28, 20122 Milano, Italy
[9] Department of Physics & Astronomy, University College London, Gower St., London, WC1E 6BT, UK
[10] Institut d'Estudis Espacials de Catalunya (IEEC), Esteve Terradas 1, Edifici RDIT, Campus PMT-UPC, 08860 Castelldefels, Spain
[11] Institute of Space Sciences, ICE-CSIC, Campus UAB, Carrer de Can Magrans, 08913, Bellaterra, Barcelona, Spain
[12] NSF NOIRLab, 950 N. Cherry Ave., Tucson, AZ 85719, USA
[13] University of California, Berkeley, 110 Sproul Hall #5800 Berkeley, CA 94720, USA
[14] Institut de Física d'Altes Energies (IFAE), The Barcelona Institute of Science and Technology, Edifici Cn, Campus UAB, 08193, Bellaterra (Barcelona), Spain
[15] Departamento de Física, Universidad de los Andes, Cra. 1 No. 18A-10, Edificio Ip, CP 111711, Bogotá, Colombia
[16] Fermi National Accelerator Laboratory, P.O. Box 500, Batavia, IL 60510, USA
[17] Sorbonne Université, CNRS/IN2P3, Laboratoire de Physique Nucléaire et de Hautes Energies (LPNHE), FR-75005 Paris, France
[18] The Ohio State University, Columbus, 43210 OH, USA
[19] Instituto de Física, Universidad Nacional Autónoma de México, Circuito de la Investigación Científica, Ciudad Universitaria, Cd. de México C. P. 04510, Mexico
[20] Departament de Física, Serra Húnter, Universitat Autònoma de Barcelona, 08193, Bellaterra (Barcelona), Spain
[21] Institució Catalana de Recerca i Estudis Avançats, Passeig de Lluís Companys, 23, 08010 Barcelona, Spain
[22] Department of Physics and Astronomy, Siena University, 515 Loudon Rd., Loudonville, NY 12211, USA
[23] Institute of Cosmology and Gravitation, University of Portsmouth, Dennis Sciama Building, Portsmouth, PO1 3FX, UK
[24] Instituto de Astrofísica de Andalucía (CSIC), Glorieta de la Astronomía, E-18008 Granada, Spain
[25] Departament de Física, EEBE, Universitat Politècnica de Catalunya, Eduard Maristany 10, 08930 Barcelona, Spain
[26] Department of Physics and Astronomy, Sejong University, 209 Neungdong-ro, Gwangjin-gu, Seoul 05006, Republic of Korea
[27] CIEMAT, Avenida Complutense 40, E-28040 Madrid, Spain
[28] Department of Physics, University of Michigan, 450 Church St., Ann Arbor, MI 48109, USA
[29] University of Michigan, 500 S. State St., Ann Arbor, MI 48109, USA
[30] National Astronomical Observatories, Chinese Academy of Sciences, A20 Datun Rd., Chaoyang District, Beijing, 100101, People's Republic of China
Received 2025 October 25; revised 2026 January 16; accepted 2026 February 6; published 2026 April 9

Abstract

On 2025 August 18, the LIGO–Virgo–KAGRA collaboration reported a subthreshold gravitational-wave candidate detection consistent with a subsolar-mass neutron star merger, denoted S250818k. An optical transient, AT2025ulz, was discovered within the localization region. AT2025ulz initially appeared to meet the expected behavior of kilonova emission, the telltale signature of a binary neutron star merger. The transient subsequently rebrightened after ∼5 days and was classified as a Type IIb supernova. In this work, we analyze the observations of its host galaxy obtained by the Dark Energy Spectroscopic Instrument (DESI). From the DESI spectrum, we obtain a secure redshift of $z = 0.084840 \pm 0.000006$. If S250818k has an astrophysical origin, this places the transient within 2σ of the gravitational-wave distance and results in an integral overlap between the gravitational-wave alert and the transient location of $\log_{10}\mathcal{I} \approx 3.9 - 4.2$. Our analysis of the host galaxy's spectral energy distribution reveals a star-forming, dusty galaxy with stellar mass $\sim 10^{10} M_{\odot}$, broadly consistent with the population of both short gamma-ray bursts and core-collapse supernova host galaxies. We also present our

[31] McWilliams Fellow.

follow-up of DESI-selected candidate host galaxies using the Fraunhofer Telescope at the Wendelstein Observatory, and show the promise of DESI for associating or rejecting candidate electromagnetic counterparts to gravitational-wave alerts. These results emphasize the value of DESI's extensive spectroscopic dataset in rapidly characterizing host galaxies, enabling spectroscopic host subtraction, and guiding targeted follow-up.

Unified Astronomy Thesaurus concepts: Galaxies (573); Time domain astronomy (2109); Gravitational waves (678); Transient sources (1851); Type II supernovae (1731)

1. Introduction

The multimessenger astronomy community has been rigorously chasing potential electromagnetic counterparts to gravitational-wave (GW) events for over a decade. The watershed discovery of the binary neutron star (BNS) merger GW signature GW170817 (B. P. Abbott et al. 2017) with its associated short gamma-ray burst (sGRB; A. Goldstein et al. 2017; V. Savchenko et al. 2017) and kilonova (KN; e.g., I. Arcavi et al. 2017; D. A. Coulter et al. 2017; M. R. Drout et al. 2017; P. A. Evans et al. 2017; M. Soares-Santos et al. 2017; E. Troja et al. 2017) provided critical insights into compact binary mergers. Despite significant follow-up efforts and some candidate counterpart reports with uncertain associations, it has been eight years since the discovery of GW170817 and the community has yet to confidently associate a second electromagnetic counterpart to a GW source, including in the ongoing fourth observing run (O4) of the LIGO–Virgo–KAGRA (LVK) collaboration. Based on the dearth of high-significance BNS merger detections since GW170817 and GW190425, the inferred rate of BNS mergers has steadily decreased with each subsequent LVK observing run (R. Abbott et al. 2023; The LIGO Scientific Collaboration et al. 2025).

On 2025 August 18, a low-significance GW candidate S250818k was detected by LVK (Ligo Scientific Collaboration et al. 2025). The signal was estimated to have a probability of being a terrestrial artifact of 71% and a 29% chance of resulting from a BNS merger (Ligo Scientific Collaboration et al. 2025). Assuming the event is of astrophysical origin, there is a >99% probability that the event involved at least one object consistent in mass with a neutron star, and that it disrupted material outside of the remnant object.[32] Moreover, given that the chirp mass is $<0.87\,M_\odot$ (Ligo Scientific Collaboration et al. 2025), there is significant probability that at least one of the two objects has subsolar mass, rendering this source particularly interesting. The Zwicky Transient Facility (ZTF) followed up part of the sky localization of S250818k and identified a candidate optical counterpart, AT2025ulz (see Figure 1; R. Stein et al. 2025). The candidate counterpart subsequently rapidly faded and reddened over the first few days (M. Busmann et al. 2025a; X. J. Hall et al. 2025a; D. A. Perley et al. 2025), in a fashion typical of a KN (X. J. Hall et al. 2025b; M. M. Kasliwal et al. 2025). Indeed, X. J. Hall et al. (2025b) find that the early-time observations can be well described by existing KN models. The identification of the source as a KN is called into question by its short-lived decay, which plateaued after a few days. The subsequent rise occurred in the fashion of a supernova (SN) (S. Banerjee et al. 2025b; R. L. Becerra et al. 2025; J. Freeburn et al. 2025; J. H. Gillanders et al. 2025a). In fact, spectroscopic features typical of Type IIb SNe were quickly identified during this rising phase (S. Banerjee et al. 2025b; N. Franz et al. 2025; J. H. Gillanders et al. 2025b; M. M. Kasliwal et al. 2025; Y. H. Yang et al. 2026), while late-time X-ray and radio observations disfavor an off-axis afterglow as the source of the rebrightening (B. O'Connor et al. 2025). On the other hand, M. M. Kasliwal et al. (2025) offer a solution to relate the nature of AT2025ulz as a Type IIb SN to the GW candidate through a "superkilonova." This is a proposed scenario in which a stripped-envelope SN produces two or more neutron stars, some of which can be of subsolar mass, and produce GWs (B. D. Metzger et al. 2024). Regardless, AT2025ulz is an interesting transient with a tantalizing possible connection to S250818k. The analysis of the extensive imaging and spectroscopic dataset (X. J. Hall et al. 2025b; M. M. Kasliwal et al. 2025) is complicated by the presence of a luminous host galaxy directly underlying the transient's position and the limited availability of pre-explosion templates.

Meanwhile, the Dark Energy Spectroscopic Instrument (DESI) has been consistently building the largest spectroscopic catalog of galaxies to date, recently surpassing over 40 million spectra (E. F. Schlafly et al. 2023; DESI Collaboration et al. 2025a, 2025b). Such a catalog provides novel opportunities in transient science, e.g., the DESI Transient Survey (X. J. Hall et al. 2025c, 2026), the MOST Hosts Survey (M. T. Soumagnac et al. 2024), and characterization of the environments and large-scale structure around GW events (A. Palmese et al. 2019, 2023; W. Ballard et al. 2023; A. J. Amsellem et al. 2025). DESI offers the ability to quickly identify and eliminate or highlight candidate counterparts that either fall within or outside the volumetric region of an LVK alert. One of the most difficult aspects of real-time transient science is the separation of transient light from the hosts, especially in the case of fainter transients. While imaging templates from wide-field surveys generally exist over most of the sky in optical filters, the availability of spectroscopic templates has been substantially lacking. Long-slit spectroscopy can be contaminated by host galaxy light, depending on the position of the transient with respect to (w.r.t.) its host and their relative brightnesses. This impacts the interpretation of transient spectra (such as blackbody temperature), the identification of absorption features, and the derivation of the intrinsic line fluxes and ratios of the underlying galaxy. Pretransient DESI spectra provide an unparalleled ability to rapidly perform spectroscopic host subtraction. AT2025ulz serendipitously occurred in a galaxy drawn from DESI's sample of ∼40 million spectroscopically observed galaxies. In this Letter, we model the host galaxy using both photometry and spectroscopy, analyze its properties and compare them to those of the hosts of other transients, estimate the probability of association with the GW alert, present our follow-up observations of DESI-selected galaxies, and demonstrate the power of a high-completeness spectroscopic survey such as DESI for multimessenger astronomy.

Throughout this Letter, we report all magnitudes in the AB system, and we assume a Planck 2018 (N. Aghanim et al.

[32] https://emfollow.docs.ligo.org/userguide/content.html

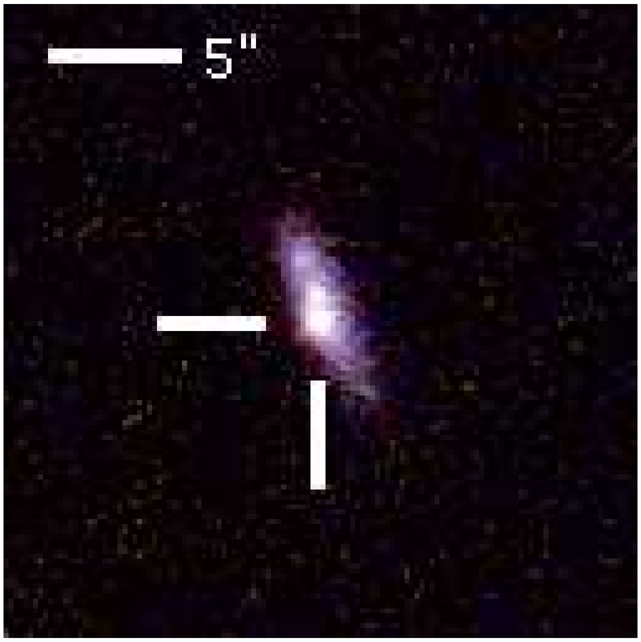

Figure 1. False-color image in *grz* bands of AT2025ulz from the first epoch of Wendelstein Observatory imaging on 2025 August 18 (M. Busmann et al. 2025a; X. J. Hall et al. 2025b). The transient is visibly off-center from the galaxy. Star-forming regions of the galaxy are noticeable as bluer patches. In this color image the transient is visually enhanced by coadding with a difference image with respect to Legacy Survey data (A. Dey et al. 2019).

2020) cosmology with the following parameters: $H_0 = 67.66\,\mathrm{km\,s^{-1}\,Mpc^{-1}}$, $\Omega_m = 0.30966$, $T_{\mathrm{CMB}} = 2.7255$ K, $N_{\mathrm{eff}} = 3.046$, $m_\nu = [0.0, 0.0, 0.06]$ eV, and $\Omega_b = 0.04897$.

2. Dark Energy Spectroscopic Instrument

DESI is comprised of 5000 fibers that can each be positioned independently on the sky (C. Poppett et al. 2024). Each fiber is 107 μm in diameter, which is equivalent to $\sim 1\overset{\prime\prime}{.}5$ on the sky. The spectrograph utilizes three cameras in the approximate *BRZ* bands that cover 3600–9824 Å at a spectral resolution $R \sim 2000$–5500 (DESI Collaboration et al. 2016, 2022, 2025a, 2025b; T. N. Miller et al. 2024). Each spectrum is reduced and the flux calibrated with the DESI spectroscopic data pipeline (J. Guy et al. 2023). To establish a redshift from a given DESI spectrum, a decomposition into a combination of template spectra is performed using Redrock[33] and a redshift is determined based on minimizing χ^2 (S. Bailey et al. 2026, in preparation). As part of DESI's Bright Galaxy Survey (C. Hahn et al. 2023), the host galaxy of AT2025ulz was observed on 2023 March 19 and is part of DESI Data Release 2 (DR2; DESI Collaboration et al. 2025a, 2025b). Given the multiple host lines and relatively high resolution of DESI ($R \sim 5000$), Redrock is able to derive a precise redshift of $z = 0.084840 \pm 0.000006$ (see Figure 7 in Appendix A).

3. Spectral Analysis

3.1. `FastSpecFit`

We measure the rest-frame optical emission-line fluxes, equivalent widths, and line ratios of the AT2025ulz host galaxy using `FastSpecFit` (version 3.2.0; J. Moustakas et al. 2023; J. Moustakas et al. 2026, in preparation; see Figure 7). `FastSpecFit` performs a joint (simultaneous) fit of the DESI three-camera optical spectrophotometry and the broadband optical plus infrared photometry from the DESI Legacy Imaging Surveys Data Release 9 (A. Dey et al. 2019). We model the stellar continuum as a nonnegative least-squares sum of five solar-metallicity, logarithmically spaced age bins between 15 Myr and 12.7 Gyr and a $\tau \propto \lambda^{-0.7}$ dust law. We then subtract the stellar continuum model from the DESI spectrum and measure all the emission lines in the observed spectral range as using constrained Gaussian line profiles. We estimate the uncertainties on the continuum and emission-line parameters using 1000 Monte Carlo realizations of the data for the host of AT2025ulz and 50 for the GRB-KN hosts. The final results are presented in Table 1 with the plotted spectrum against the modeled one in Appendix A, Figure 7. One noteworthy component of AT2017gfo was the active galactic nucleus (AGN) activity of the host (A. Palmese et al. 2017). To determine if such weak AGN lines are present in the host of AT2025ulz, we perform a Baldwin–Phillips–Terlevich (BPT; J. A. Baldwin et al. 1981) analysis (Figure 2). We determine that the emission lines are more consistent with those of a purely star-forming galaxy, similar to known GRB-KN also in DESI.

Table 1
Emission Line Measurements and Ratios for the AT2025ulz Host Galaxy Based on the `FastSpecFit` Run

Quantity	Value
z	0.084840 ± 0.000006
EW(Hα) [Å]	22.72 ± 0.66
EW([O II]) [Å]	19.6 ± 3.75
EW([O III]) [Å]	2.14 ± 0.30
Hα/Hβ	4.67 ± 0.48
$\log_{10}$([O III] λ5007/Hβ)	−0.33 ± 0.07
$\log_{10}$([N II] λ6584/Hα)	−0.53 ± 0.03
$\log_{10}$([S II] λ6716/Hα)	−0.57 ± 0.04
[O II] λ3726/λ3729	0.66 ± 0.18
[S II] λ6731/λ6716	0.57 ± 0.10
A_V [mag]	1.302 ± 0.272
SFR [$M_\odot$ yr^{-1}]	0.386 ± 0.104

Notes. The A_V extinction is computed from the Balmer decrement with the Calzetti Milky Way dust law with $R_V = 3.1$ (D. Calzetti et al. 1994). We compute the star formation rate using Equation (2) from E. J. Murphy et al. (2011).

3.2. `prospector`

The complete spectral energy distribution (SED) is also modeled with `prospector` (J. Leja et al. 2017; B. D. Johnson et al. 2019, 2021). For this fit, we use photometry based on the R. G. Kron (1980) radius produced by `HostPhot` (T. Müller-Bravo & L. Galbany 2022). We derive a Kron radius from *grz* imaging from the Legacy Survey (A. Dey et al. 2019) and apply that aperture to far-UV and near-UV imaging from the Galaxy Evolution Explorer (L. Bianchi et al. 2017), *ugriz* imaging from the Sloan Digital Sky Survey (R. Ahumada et al. 2020), $grizy_{P1}$ imaging from Pan-STARRS (N. Kaiser et al. 2010; K. C. Chambers et al. 2016), and J, H, and K_s imaging from the Two Micron All Sky Survey (2MASS; M. F. Skrutskie et al. 2006). Due to the vast pixel difference in mid-IR imaging, we fit a new

[33] https://github.com/desihub/redrock/

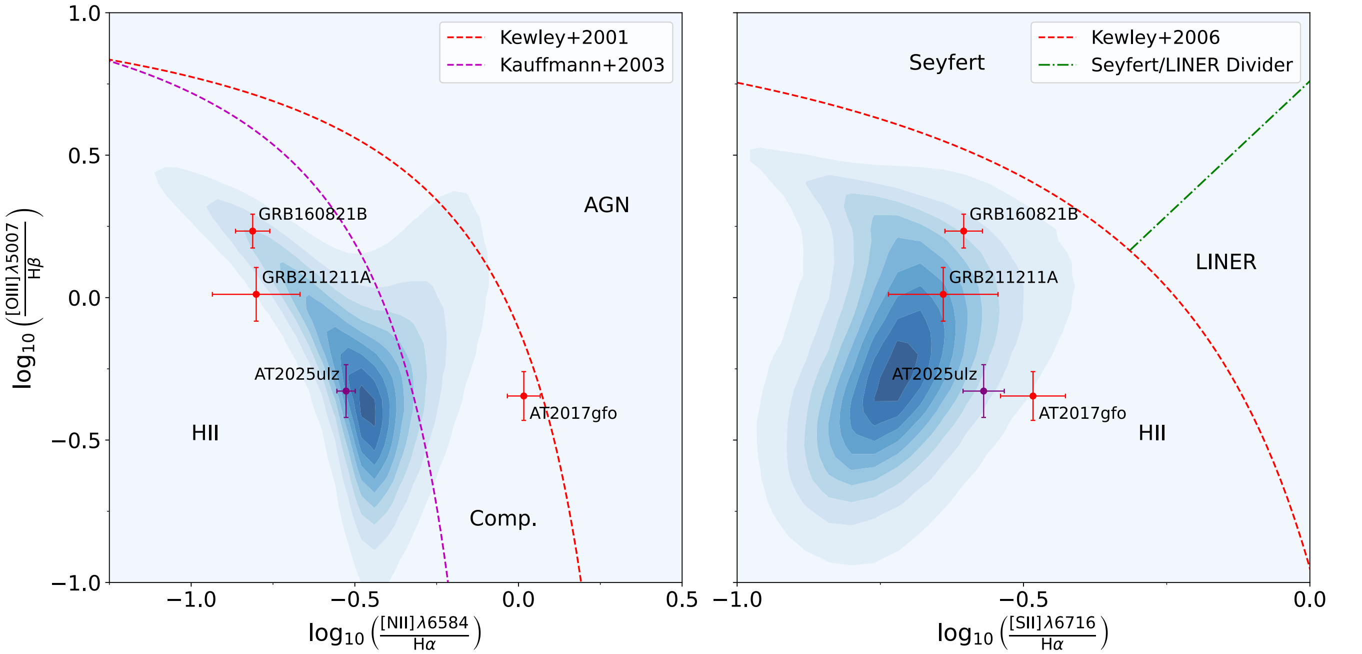

Figure 2. A BPT (J. A. Baldwin et al. 1981) analysis of the host of AT2025ulz (violet) based on its DESI spectrum and including for comparison the host galaxies of known gamma-ray bursts with an associated candidate KN (GRB160821B and GRB211211A) observed by DESI. The galaxy is a standard star-forming galaxy, similar to the hosts of known GRB-KN. Notably, the host of AT2017gfo (associated with GW170817) has weak AGN lines that are not present in any of the other galaxies (A. Palmese et al. 2017). The background contours are made from the `FastSpecFit` value-added catalog for DESI DR2 data (`FastSpecFit` version 3.2.0; J. Moustakas et al. 2023; DESI Collaboration et al. 2025b; J. Moustakas et al. 2026, in preparation). Separation lines are drawn from L. J. Kewley et al. (2001), G. Kauffmann et al. (2003), and L. J. Kewley et al. (2006).

Kron radius for W1 and apply it to all imaging from the Wide-field Infrared Survey Explorer (WISE; E. L. Wright et al. 2010). All photometry is corrected for Milky Way extinction using dust maps from E. F. Schlafly & D. P. Finkbeiner (2011) and the extinction curve from E. L. Fitzpatrick (1999).

A parametric delayed-τ star formation history is used, with the timescale τ drawn from a log-uniform prior between 0.1 and 10 Gyr. The main stellar population parameters, including total mass M, age $t_{\rm age}$, e-folding time τ, stellar metallicity $\log Z/Z_\odot$, and dust attenuation A_V, are given broad uniform priors. A Chabrier initial mass function is assumed (G. Chabrier 2003) and dust attenuation is modeled with the Calzetti Milky Way dust law with $R_V = 3.1$ (D. Calzetti et al. 1994). Furthermore, we do not model various stellar emission lines. The galaxy's redshift is fixed to the spectroscopic value of $z = 0.084840$. The stellar continuum is supplemented with hot dust emission (B. T. Draine & A. Li 2007) and with an AGN-heated dust component allowed to contribute a fraction $f_{\rm AGN}$ of the total bolometric stellar luminosity of the galaxy (M. Nenkova et al. 2008). Given the posterior samples provided by `prospector`, we report the median galaxy properties in Table 2. Furthermore, for errors, we report the 16th and 84th percentiles of the posterior sample. From the derived posteriors on M, $t_{\rm age}$, and τ we compute the stellar mass M_*, star formation rate (SFR), and mass-weighted stellar age t_m using the standard formulae (B. D. Johnson et al. 2019). The best-fit SED is shown in Figure 3 and a corner plot is shown in Appendix A, Figure 6. The derived parameters are in general agreement with the host galaxy modeling presented by J. H. Gillanders et al. (2025b).

Table 2
Median and 16th and 84th Percentiles of AT2025ulz's Host Galaxy Parameters Based on Our `prospector` Modeling

Parameter	Value
$\log(M_*/M_\odot)$	$9.92^{+0.13}_{-0.15}$
$\log(Z/Z_\odot)$	$-0.72^{+0.23}_{-0.25}$
A_V [mag]	$0.32^{+0.09}_{-0.10}$
$t_{\rm age}$ [Gyr]	$6.04^{+3.96}_{-2.74}$
τ [Gyr]	$1.23^{+0.88}_{-0.63}$
$\log(f_{\rm AGN})$	$-1.58^{+0.22}_{-0.34}$
SFR [$M_\odot$ yr^{-1}]	$0.52^{+0.15}_{-0.16}$
t_m [Gyr]	$3.83^{+2.36}_{-1.66}$

4. Comparison of the Host Galaxy Properties to sGRB and Core-collapse Supernova Hosts

According to the BPT analysis (Figure 2), the host of AT2025ulz appears to fall squarely within the star-forming regime. This is in line with the fact that there is minimal AGN contribution found by the `prospector` fit (Table 2, with an AGN fraction of ∼0.021). The data here then suggest that the spectrum of the host of AT2025ulz is dominated by ongoing star formation rather than nuclear activity, consistent with what is typically observed in galaxies hosting core-collapse (CC) SNe and sGRBs.

This is noticeably different from the host of GW170817 (NGC 4993; see Figure 3 of A. Palmese et al. 2017). The galaxy there is markedly different, being an early-type system with an old stellar population and low star formation activity. Perhaps most uniquely, the host galaxy of GW170817 also has clear evidence of a recent galactic merger. The list of merger signatures includes disturbed stellar light profiles and kinematic

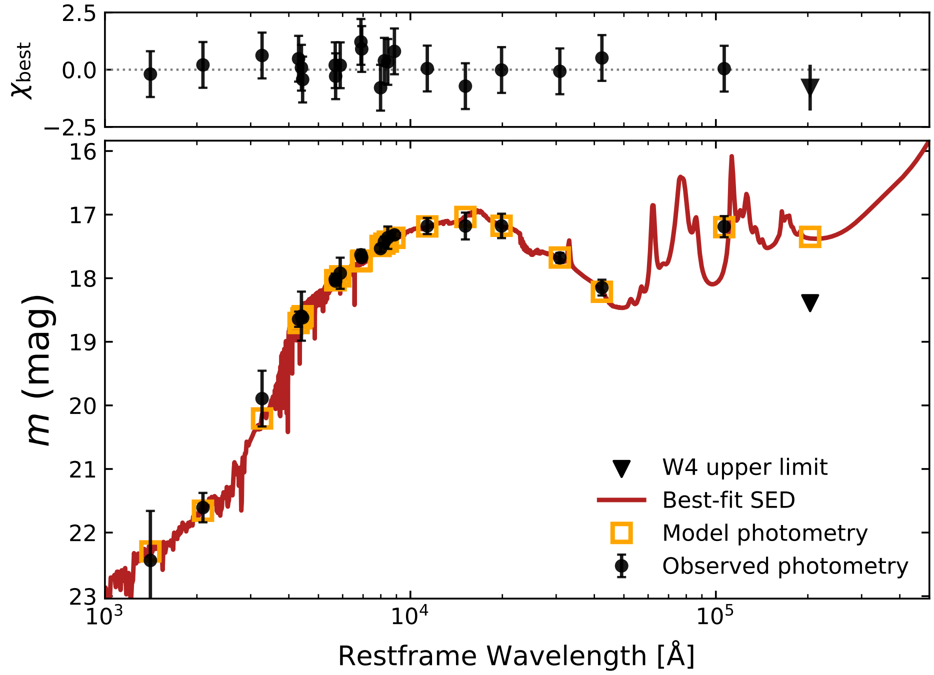

Figure 3. The best-fit host galaxy SED derived using `prospector` (B. D. Johnson et al. 2019). Model photometry is shown as orange squares and compared to the observed photometry (black circles). The top panel shows the residuals compared to the best-fit SED (red line).

peculiarities in observations. Such a merger event may have influenced the formation of the binary system, a mechanism that would be missing in the case of the host of AT2025ulz, at least based on the available data. Note however that the specific SFR (sSFR) of the GW170817 host is in the low-end tail of the sGRB host population, and hence atypical even for those kinds of transients. In general, given the significantly higher SFR for the host of AT2025ulz compared to NGC 4993, the transient is more likely related to a formation pathway with shorter time delay than GW170817.

Theoretical models have suggested that the formation of subsolar-mass neutron star mergers in the accretion disk of a collapsar is possible (A. L. Piro & E. Pfahl 2007; B. D. Metzger et al. 2024; Y.-X. Chen & B. D. Metzger 2025; Y. Lerner et al. 2026). As AT2025ulz is suggested to be linked to both BNS mergers and Type IIb SNe (M. M. Kasliwal et al. 2025), we compare the host galaxy properties to those of the host galaxies of CC SNe (S. Schulze et al. 2021) and sGRBs (A. E. Nugent et al. 2022; B. O'Connor et al. 2022). We additionally highlight the host galaxies of sGRBs with candidate KN associations, referred to as GRB-KN (A. Gal-Yam et al. 2006; E. Berger et al. 2013; N. R. Tanvir et al. 2013; Z.-P. Jin et al. 2016; E. Troja et al. 2018, 2019; 2022; W. Fong et al. 2021; B. O'Connor et al. 2021; J. C. Rastinejad et al. 2022; A. Levan et al. 2024; Y.-H. Yang et al. 2024). We limit our comparison to galaxies at $z < 0.6$. Figure 4 shows a comparison between stellar mass and sSFR, which places the host of AT2025ulz at a typical location in either population.

We note that the SFR inferred from SED modeling is higher (by a factor of $\sim$1.35), but also within 2σ, compared to the value inferred from the Hα emission line ($0.386 \pm 0.104\ M_\odot\ \mathrm{yr}^{-1}$) even after correcting for the extinction inferred from the Balmer decrement (see Table 1). Additionally, the radio-inferred SFR ($2.07 \pm 0.26\ M_\odot\ \mathrm{yr}^{-1}$; G. Bruni et al. 2025) is higher than that (by a factor of $\sim$4), suggesting dust-obscured star formation in the host galaxy. This is reasonable to consider as the galaxy is

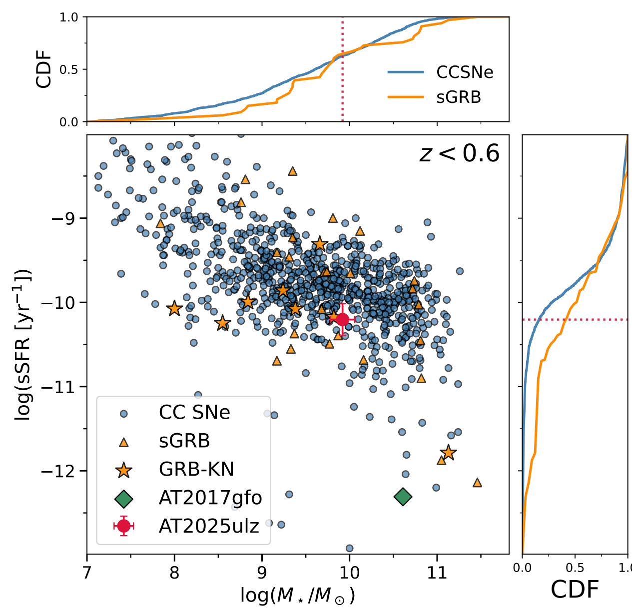

Figure 4. A comparison of the sSFR versus stellar mass of CC SNe (S. Schulze et al. 2021), sGRBs (A. E. Nugent et al. 2022; B. O'Connor et al. 2022), GRB-KN (A. Gal-Yam et al. 2006; Z.-P. Jin et al. 2016; J. C. Rastinejad et al. 2022; E. Troja et al. 2022; A. Levan et al. 2024; Y.-H. Yang et al. 2024), AT2017gfo (A. Palmese et al. 2017; A. E. Nugent et al. 2022), and the host of AT2025ulz (see Table 2). We have limited the redshift of all events shown here to $z < 0.6$ for comparison to the highest-z GRB-KN candidate (GRB200522A at $z = 0.554$; W. Fong et al. 2021; B. O'Connor et al. 2021). The position of AT2025ulz's host is consistent with both CC SNe and sGRBs.

found to be quite dusty from both emission-line diagnostics and the SED modeling. Both the Hα and radio SFRs are inferred following E. J. Murphy et al. (2011). It is also possible that this difference is due to mismatches between the size of the DESI fiber (which does not capture the entire galaxy) and the size of

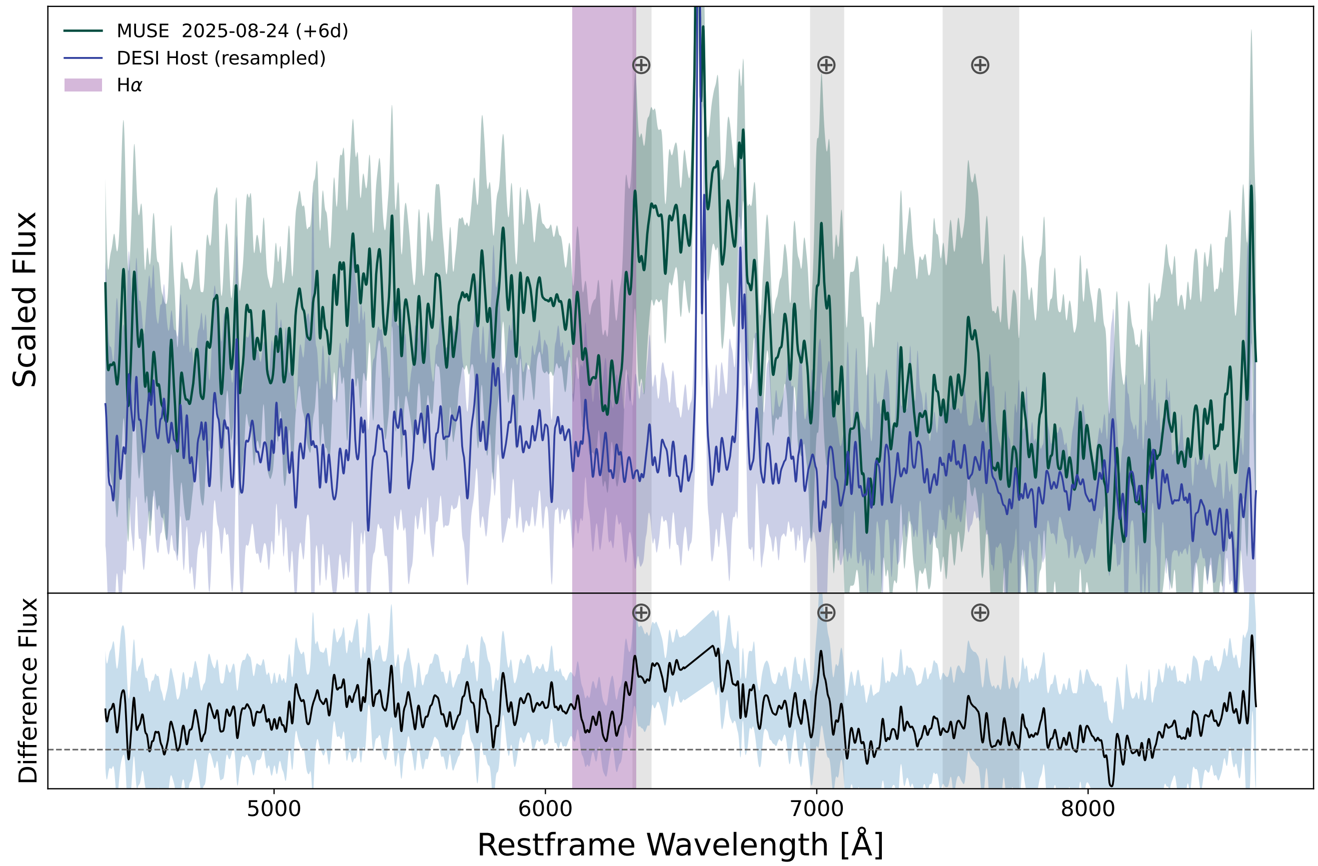

Figure 5. MUSE spectrum of AT2025ulz reported by S. Banerjee et al. (2025a) and DESI host spectrum of AT2025ulz. The MUSE spectrum classifies AT2025ulz as a Type IIb SN. The top panel shows both spectra normalized by their median flux while the bottom panel shows the MUSE spectrum with the DESI spectrum subtracted. Tellurics are denoted with ⊕ and the Hα and N II complex is masked out in the subtraction. A clear P Cyg Hα shape can be seen.

the extended stellar population of the host galaxy, whereas both the host galaxy photometry and radio emission can capture the full extent (size) of ongoing star formation. Additionally, radio emission traces star formation on longer timescales ∼100 Myr compared to the shorter timescale ∼10 Myr traced by Hα (e.g., J. J. Condon 1992; R. C. Kennicutt & N. J. Evans 2012; D. Calzetti 2013). Therefore, the deviation in the optically inferred SFR and radio-inferred SFR may be either due to dust obscuration (above what is derived from the Balmer decrement) or a poststarburst episode with a rapidly declining SFR in the last ∼100 Myr.

5. Host Subtraction

Host subtraction is a difficult but important task in transient astronomy. While host subtraction with photometry is relatively straightforward, spectroscopic host subtraction is considerably more challenging for two reasons: the subtraction process itself is nontrivial, and suitable host galaxy template spectra are often unavailable. Even with sufficient templates, instrumental issues with different resolution, apertures, slit losses, telluric corrections, and flux calibrations cause further difficulty. Thus proposed is a straightforward and effective method to highlight broad lines in various spectra. A simple demonstration that this methodology is suitable can be found in Appendix B. The processes involves convolving spectra to a common resolution, then rebinning with interpolation to a common wavelength bin. In this case, the DESI spectrum is rebinned to the spectrum taken by MUSE (S. Banerjee et al. 2025a, 2025b) approximately 6 days after the GW event. After binning, the spectra are normalized by the median flux over the common wavelength grid and then subtracted. The results of such a subtraction can be seen in Figure 5. In both the original and subtracted spectra, we can see the presence of a P Cyg Hα line (as noted in S. Banerjee et al. 2025a), which is a telltale sign of a Type II or IIb SN (see also N. Franz et al. 2025; J. H. Gillanders et al. 2025b; Y. H. Yang et al. 2026). Host subtraction is important: if this event was a KN, host subtraction could elucidate the heavy metal lines that indicate *r*-processing and would prove a telltale sign of a KN event.

6. DESI Redshifts of Candidates

6.1. Probability of Association with S250818k given the AT2025ulz Host Redshift

To assess whether AT2025ulz is potentially associated with the GW candidate S250818k, we compute the probability that its host galaxy lies within the 3D localization volume of the event. Following the formalism described in G. Ashton et al. (2018), we use the latest and publicly available BILBY (G. Ashton et al. 2019) localization skymap (L. P. Singer et al. 2016) encoding the posterior density over sky position and luminosity distance, which can be factorized as

$$p(\alpha, \delta, d_L) = p(d_L|\alpha, \delta)\, p(\alpha, \delta), \qquad (1)$$

where $p(\alpha, \delta)$ is the marginalized sky probability and $p(d_L|\alpha, \delta)$ is the conditional distance posterior along each line of sight. The odds of association are given by the overlap integral defined as

$$\mathcal{I} = \int \frac{p(d_L(z_{\rm EM})|\alpha_{\rm EM}, \delta_{\rm EM})p(\alpha_{\rm EM}, \delta_{\rm EM})}{\pi(\alpha_{\rm EM}, \delta_{\rm EM})} d\alpha_{\rm EM}\, d\delta_{\rm EM}, \quad (2)$$

where $\pi(\alpha_{\rm EM}, \delta_{\rm EM})$ is the probability for the position of the transient to have originated from a random association and where ($\alpha_{\rm EM}$, $\delta_{\rm EM}$, $z_{\rm EM}$) correspond to the AT2025ulz host galaxy position. We find $\log_{10}\mathcal{I} \approx 3.9 - 4.2$ depending on the value of the Hubble constant we use. For comparison purposes, the overlap integral for GW170817 and its host galaxy NGC 4993 is $\log_{10}\mathcal{I} \sim 5.6$ (B. Piotrzkowski et al. 2022). To interpret these odds, we compare them against the following null hypotheses: a galaxy is drawn uniformly in comoving volume and uniformly on the sky with no distance information. The uniform-in-comoving-volume prior corresponds to the expectation for a random galaxy population, while the uniform-sky prior corresponds to the chance alignment of a transient with the 2D localization region. The ratio of the measured overlap to these null expectations provides an odds ratio for association versus random chance of coincidence. However, as emphasized in prior work (G. Ashton et al. 2021; M. Bhardwaj et al. 2024; I. Magaña Hernandez et al. 2024), spatial and distance consistency are necessary but not sufficient conditions for association: a robust claim requires a physical model that explains the transient's observed evolution in the context of a compact binary merger (e.g., M. M. Kasliwal et al. 2025). However, even such a physical explanation must be interpreted while accounting for the low likelihood that the gravitational event is astrophysical in origin.

6.2. Other Candidates

Based on the tentative association of AT2025ulz with the GW candidate, we also report here DESI's contribution to the follow-up of S250818k for other identified transients. We perform a crossmatch of all candidates that were discovered after the GW event and positionally coincident transients to S250818k reported publicly on the Transient Name Server (TNS) to the current DESI catalog as of 2025 September 26. In order to perform this crossmatch, first we find the three most probable hosts of any given transient using the projected distance from the host nucleus. We identify the most probable host in the Legacy Survey DR9 (A. Dey et al. 2019) using the directional light radius method (M. Sullivan et al. 2006; M. Smith et al. 2020). From this, we retain only convincing sources in Legacy Survey DR9 for host identification that satisfy two criteria: (1) robust detections in at least two of the *grz* bands with $g < 24$, $r < 23.4$, and $z < 22.5$, and (2) physically plausible colors, restricted to $-1 < g - r < 4$. This permits the search of transients that are potentially very off-nuclear and broadens the set of potential sources.

To further demonstrate the potential of such a DESI crossmatch when combined with advanced scanning tools, we take the 121 candidates presented in Table 3 of N. Franz et al. (2025), which is a list of all TNS candidates discovered within 5 days of the GW candidate within the GW alert area. Of these 121 transients, 51 have DESI redshifts. Of those redshifts, we can exclude 43 using the DESI catalog on the basis of distance alone leaving only eight viable candidates. The DESI catalog, combined with this novel scanning method, could automatically exclude 35% of the candidates. More importantly, we identify two candidates 2025utx and 2025uxs which have photometric redshifts of 0.13 (R. Beck et al. 2016) and 1.02 (H. Zou et al. 2019). Such photometric redshifts would disqualify them from selection; however, their DESI spectroscopic redshifts are approximately $z = 0.08$ and 0.06, respectively, and thus they are within the GW event volume (see Table 4 in Appendix C). This emphasizes that photometric redshifts can be unreliable and spectroscopic redshifts from DESI can be crucial to candidate vetting. Indeed we also look at the "high-scoring" (score > 0.35) candidates from N. Franz et al. (2025), and can immediately exclude three of five transients: two are too distant (AT2025uua and AT2025uus; see Table 5 in Appendix C) and one (AT2025usl) is in the volume but can be excluded based on the public ZTF forced photometry (F. J. Masci et al. 2023). The two remaining transients (AT2025uow and AT2025uuf) are outside of the DESI footprint.

For completeness, there have been 152 transients reported to TNS within the 99% confidence region of S250818k.[34] We find DESI redshifts for 73 of these transients. We inspect the 15 for which the matches are within the volume, i.e., the DESI redshift is consistent, and find that 13 out of 15 have correctly matched hosts as indicated by an eye inspection of whether the transient seems the best match to the DESI host and are within the volume. We compile the following candidates with redshifts that are within the 3σ space given Planck cosmology (N. Aghanim et al. 2020) in Table 4. Candidates that are outside the volume can be rejected as unrelated to the GW event. Those 58 transient candidates that are outside the reported volume can be found in Appendix C in Table 5.

7. Targeted Follow-up of DESI-selected Hosts

A third strategy in which DESI spectroscopic redshifts guide follow-up efforts of GW events is that they enable the identification of host galaxies whose 3D position best matches the GW localization volume. With the coverage of DESI spectroscopy, particularly from the Bright Galaxy Survey, wide-field spectroscopy enables pinpointing the redshifts of the majority of the stellar mass in the range where BNS events are detectable by LVK. Targeted, deep follow-up with instruments that have only a limited field of view (FOV) can then cover the actual host with substantial probability in the case of well-localized GW events.

We utilized this strategy, too, in the case of S250818k. From the latest catalog of DESI redshifts, we selected those 20 galaxies in the northern hemisphere part of the LVK localization region of S250818k that maximized the product of 3D probability density and stellar mass (see Appendix D for more details). In this, we marginalized over the uncertainty in cosmological parameters when converting redshift to luminosity distance (based on a broad uniform prior between the SH0ES (A. G. Riess et al. 2022) and Planck (N. Aghanim et al. 2020) Hubble constant constraints), and used the Legacy Survey *z*-band flux as a stellar mass proxy.

Follow-up of these candidate hosts commenced on 2025 August 19 21:50 UT. Observations were conducted with the Fraunhofer Telescope at Wendelstein Observatory (FTW; U. Hopp et al. 2014) using the Three Channel Imager (3KK; F. Lang-Bardl et al. 2016). We simultaneously imaged the *r*, *z*,

[34] https://www.wis-tns.org/ligo/o4/S250818k_20250818_012006

and J bands for 3×180 s on each of the first 10 potential host galaxies selected as described above, ordered by observability. The list of targets observed is provided in Appendix B.

The images were reduced using a custom pipeline (see C. A. Gössl & A. Riffeser 2002; M. Busmann et al. 2025b for details). Astrometry was calibrated by matching to the Gaia catalog (Gaia Collaboration et al. 2021). We used the Pan-STARRS DR1 catalog (N. Kaiser et al. 2010) to determine zero-points of the r- and z-band images, and the 2MASS catalog (M. F. Skrutskie et al. 2006) for the J band.

At the time of observations, 1.85 days post the GW event, a hypothetical KN would have been close to the peak of its red-optical emission. At the typical photometric depths achieved for point sources, $r \approx 23.3$, $z \approx 22.0$, and $J \approx 21.5$ mag (3σ, AB), such a transient would be detectable at high significance according to both models and afterglow-KNe in the literature (e.g., X. J. Hall et al. 2025b). The FOV of the instrument is also suitable for this search: at the distance of $d_L = 259$ Mpc, the 7' FOV of the 3KK instrument results in physical distances of more than 200 kpc from the center being observed, easily covering the full range of offsets of GRB-KN from galactic centers (W.-f. Fong et al. 2022; B. O'Connor et al. 2022).

We performed difference imaging of the r and z bands relative to Legacy Survey imaging. Visual inspection of the images did not reveal any candidate transient in our data. We repeated difference imaging analysis in the r, z, and J bands against template images we took ourselves on 2025 October 2, after the decay of a hypothetical transient. Here, too, no transient was detected.

8. Conclusion

In this work, we provide the properties of the host of the transient AT2025ulz, hypothesized to be a candidate counterpart to the GW event S250818k (X. J. Hall et al. 2025b; M. M. Kasliwal et al. 2025). We also reduce the list of other potential counterparts, based on DESI spectroscopic redshifts that place their hosts outside the GW event localization, and present the follow-up carried out around DESI potential host galaxies with the 2.1 m FTW.

One novel advantage of DESI's extensive redshift catalog is the ability to rapidly identify the most promising transients for further observations during GW event follow-up campaigns. Having an immediate, precise redshift reference allows observers to quickly reject candidates that lie outside the localization volume or that exhibit absolute magnitudes inconsistent with a KN. For the case of AT2025ulz, we measure an integral overlap of $\log_{10} \mathcal{I} \approx 3.9 - 4.2$, which, based on the 3D location of this transient w.r.t. the GW candidate, supports its possible association, although the estimated statistic does not account for the physical interpretation of the transient emission as arising from the GW source, nor the probability of S250818k being of astrophysical origin. This capability significantly improves the efficiency of follow-up efforts by narrowing the field to likely counterparts. In the case of S250818k alone, hundreds of transients have been discovered within the sky localization region (N. Franz et al. 2025; J. H. Gillanders et al. 2025b; M. M. Kasliwal et al. 2025). Roughly half of these already had a redshift associated with their likely respective host galaxy in DESI. A crucial component of GW follow-up is not only the identification of the true counterpart, but also the confident rejection of all other candidates. Since it is impractical to maintain rigorous follow-up of every transient, DESI's redshift catalog represents a major advance in our ability to prioritize and eliminate candidates effectively.

Another critical use of DESI is the ability to perform spectroscopic host subtraction, revealing the intrinsic transient spectrum and minimizing host contamination to feature identification. As demonstrated (Figure 5), host subtraction is required for both detecting broad features found in spectra and determining the continuum color of transient spectra. Further work into building a more rigorous method to use DESI spectra to produce host-subtracted spectra is warranted. Such an approach could involve using time-concurrent and historic photometry to better constrain both continuum and transient properties. Galactic properties vary over the face of the entire galaxy; by taking photometry at a fiber-size aperture compared to the nucleus (where the DESI spectrum is taken) one could recalibrate the continuum and then when subtracting use difference photometry to calibrate the subtracted spectrum. Such rigor in spectral subtractions will prove essential for the discovery of these intrinsically faint compact object mergers. If in the future more candidates are found within bright galaxies, it will be equally essential to remove the contaminating galaxy light.

While galaxy-targeted searches for the electromagnetic counterparts of GW events are a regular occurrence in the last decade (e.g., N. Gehrels et al. 2016), these searches can suffer from the limited completeness of spectroscopic galaxy catalogs as the GW event horizon continues to increase. The vast scale of the complete DESI catalog means that even with candidates of moderate localization, the redshift of a large fraction of possible host galaxies will be known ahead of time. Thus, dedicated observations of high-probability in-volume candidate host galaxies offer a new potential path for a smaller class of telescopes in the era of the Vera C. Rubin Observatory. As the LVK detectors are upgraded and next-generation GW detectors come online, the distance and hence the typical apparent magnitude of electromagnetic counterparts to compact mergers will be out of reach for many wide-field surveys with smaller apertures than Rubin (e.g., R. Kaur et al. 2026; K. Kunnumkai et al. 2025a, 2025b). However, through deep observations of high-probability hosts, we will be able to better leverage smaller telescopes to discover these faint and distant events.

With the end of LIGO O4c and the imminent onset of the Vera C. Rubin Observatory Legacy Survey of Space and Time (LSST), it is crucial to continue efforts to uncover these rare but fascinating compact binary mergers. Leveraging spectroscopic galaxy catalogs to conduct rigorous searches for orphan KNe will be essential for building a robust sample that can be further expanded with the future LVK O5 or A# events.

Acknowledgments

The authors thank the anonymous referee for useful comments that improved the manuscript. X.J.H. thanks Noah Franz for providing greater detail on his work, and providing tables regarding the host galaxies of transients identified with his novel pipeline (N. Franz et al. 2025).

This work is supported by NSF grant No. 2308193. B.O. is supported by the McWilliams Postdoctoral Fellowship in the McWilliams Center for Cosmology and Astrophysics at Carnegie Mellon University. This material is based on work supported by the U.S. Department of Energy (DOE), Office of

Science, Office of High-energy Physics, under contract No. DE-AC02-05CH11231, and by the National Energy Research Scientific Computing Center, a DOE Office of Science User Facility under the same contract. Additional support for DESI was provided by the U.S. National Science Foundation (NSF), Division of Astronomical Sciences under contract No. AST-0950945 to the NSF's National Optical-infrared Astronomy Research Laboratory; the Science and Technology Facilities Council of the United Kingdom; the Gordon and Betty Moore Foundation; the Heising-Simons Foundation; the French Alternative Energies and Atomic Energy Commission (CEA); the National Council of Humanities, Science and Technology of Mexico (CONAHCYT); the Ministry of Science, Innovation and Universities of Spain (MICIU/AEI/10.13039/501100011033); and the DESI Member Institutions: https://www.desi.lbl.gov/collaborating-institutions. Any opinions, findings, and conclusions or recommendations expressed in this material are those of the authors and do not necessarily reflect the views of the U.S. National Science Foundation, the U.S. Department of Energy, or any of the listed funding agencies.

The authors are honored to be permitted to conduct scientific research on I'oligam Du'ag (Kitt Peak), a mountain with particular significance to the Tohono O'odham Nation.

This Letter contains data obtained at the Wendelstein Observatory of the Ludwig Maximilian University of Munich. Funded by the Deutsche Forschungsgemeinschaft (DFG, German Research Foundation) under Germany's Excellence Strategy—EXC-2094—390783311.

This work used resources on the Vera Cluster at the Pittsburgh Supercomputing Center (PSC). Vera is a dedicated cluster for the McWilliams Center for Cosmology and Astrophysics at Carnegie Mellon University. We thank the PSC staff for their support of the Vera Cluster.

This publication makes use of data products from the Wide-field Infrared Survey Explorer, which is a joint project of the University of California, Los Angeles, and the Jet Propulsion Laboratory/California Institute of Technology, funded by the National Aeronautics and Space Administration.

This publication makes use of data products from the Two Micron All Sky Survey, which is a joint project of the University of Massachusetts and the Infrared Processing and Analysis Center/California Institute of Technology, funded by the National Aeronautics and Space Administration and the National Science Foundation.

Facilities: Mayall, WO:2m

Appendix A
SED Modeling

Here we present the `prospector` (Figure 6) and `FastSpecFit` (Figure 7) modeling results of the host of AT2025ulz. For the `FastSpecFit` fit, various lines, the spectral fit, and the overall SED fit can be seen.

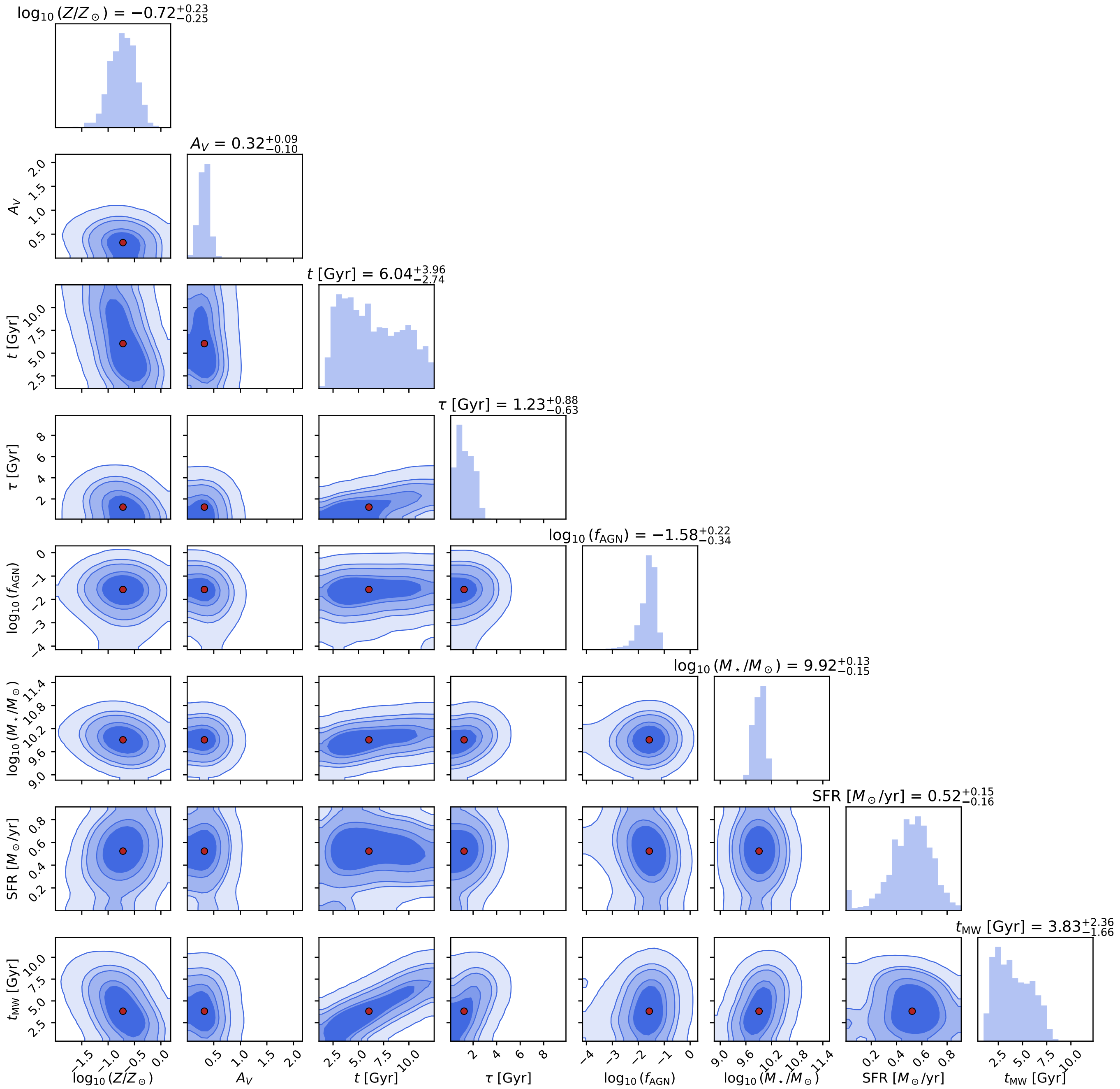

Figure 6. Corner plot showing the posterior distribution of the host galaxy parameters derived using `prospector` (B. D. Johnson et al. 2019). The median point is placed in red.

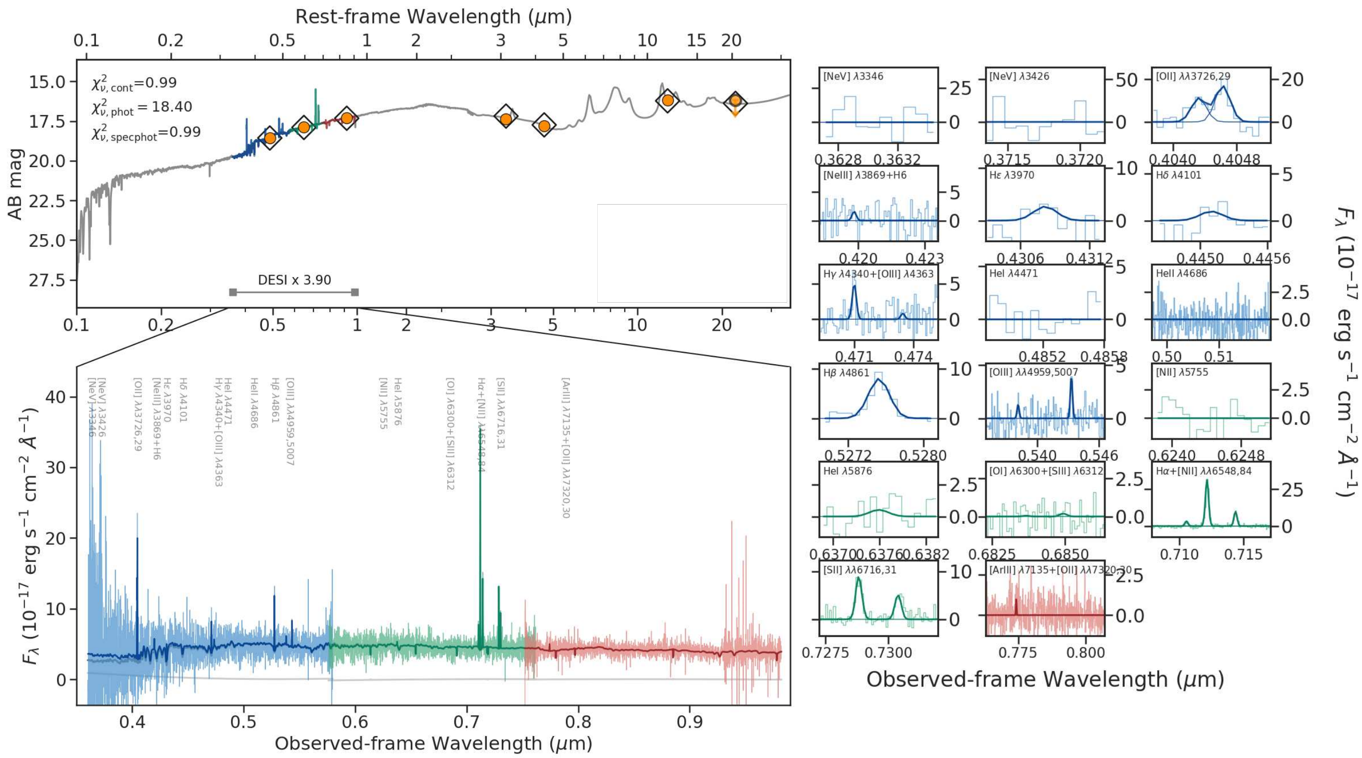

Figure 7. Left: SED fit from `FastSpecFit`, combining Legacy Survey and WISE photometry with DESI spectra. The lower panel shows the stellar population model spectrum, with key emission lines labeled. Right: Gaussian fits to individual spectral features used to measure line properties. The dark curve shows the best-fit model, while the faint lines represent the DESI data.

Appendix B
Quality of Host Subtraction

In Section 5, we use the DESI host spectra of AT2025ulz, to subtract off potential host contamination of the transient. To demonstrate the effectiveness of this method, we use Next Generation Superfit (NGSF; S. Goldwasser et al. 2022). NGSF uses a combined fit from a set of template galaxies, as well as template SNe. For this test, we force a redshift of $z = 0.08480$ and only allow NGSF to fit IIb spectra. For the unsubtracted spectrum we allow NGSF to mask galaxy lines but do not mask tellurics (since they are already corrected for). For the subtracted spectrum, we do mask tellurics as they become clear, perhaps due to an imperfect correction, but do not mask galaxy lines through NGSF (since the subtraction has already masked these). We compare the results in Table 3. It is clear that the fit χ^2 improves after the host subtraction, with the majority of the object flux being from the SN (see column Frac(SN)).

Table 3
Comparison of NGSF Results for the Original MUSE Spectrum and the Host-subtracted MUSE Spectrum

Spectrum	Frac(SN)	χ^2/dof
MUSE (original)	0.446	5.87
MUSE (host-subtracted)	0.836	3.63

Note. We report the best-fit SN flux fraction and the reduced chi-square of the fit.

Appendix C
DESI Candidates

Here we list two tables. The first table (Table 4) is a list of all transients reported to TNS within the localization of the LVK alert and having redshifts consistent with such a volume. The second table (Table 5) includes transient candidates that are rejected due to a host that is outside of the 3σ probability region provided by LVK for S250818k.

Table 4
Crossmatch of Publicly Reported Transients Temporally and Positionally Coincident with S250818k to the DESI Catalog (as of 2025-09-26)

TNS Name	R.A. Host	Decl. Host	z	D_L [Mpc]	Discovery	Note
2025uxs*	236.0596	27.4798	0.06275	291.1	K. C. Chambers et al. (2025a)	Ia SN (J. Wise et al. 2025)
2025utx*	251.0454	42.4654	0.08009	376.0	K. C. Chambers et al. (2025b)	
2025vnt*	237.5920	29.0245	0.07551	353.4	J. Sollerman et al. (2025a)	Ia SN (C. Fremling et al. 2025)
2025uzd*	251.2640	44.2982	0.06733	313.3	R. Stein (2025)	
2025utr*	271.9428	56.8697	0.05592	258.2	K. C. Chambers et al. (2025b)	
2025utq	262.9458	54.7942	0.08100	380.5	K. C. Chambers et al. (2025b)	
2025usy*	268.8042	56.0342	0.08574	404.1	K. C. Chambers et al. (2025b)	
2025uqe	258.0304	49.2303	0.07303	341.2	R. Stein (2025)	
2025upw	222.0821	9.1172	0.02921	132.3	J. Tonry et al. (2025)	
2025ulz*	237.9757	30.9026	0.08484	399.6	R. Stein et al. (2025)	IIb SN (S. Banerjee et al. 2025b)
2025uso*	244.2394	35.0560	0.02517	113.6	K. C. Chambers et al. (2025b)	IIb SN (J. Sollerman et al. 2025b)
2025unu	239.5424	42.9910	0.06114	283.3	D. O. Jones et al. (2025)	
2025wcl	36.4880	1.1867	0.07291	340.6	E. O. Ofek et al. (2025)	

Notes. We offer the publicly available classification of a transient if it is available. We mark the ones that were discovered within 5 days of the GW trigger with an *.

Table 5
Crossmatch of Transients with DESI Catalog Entries Whose Redshift Confidently Places Them outside the GW Localization Region

TNS Name	R.A. Host	Decl. Host	z	Spectype	D_L [Mpc]
2025uus	244.2946	39.6485	0.1479	GALAXY	725.8524
2025uuq	244.6472	37.9424	0.1214	QSO	586.0073
2025uul	237.0139	29.7992	0.4025	QSO	2256.6342
2025vaj	245.1992	42.0982	0.2295	GALAXY	1180.8826
2025uzl	241.6002	37.7827	0.2003	GALAXY	1013.7973
2025vaa	254.1146	46.8251	0.6117	GALAXY	3721.9598
2025uzx	242.0437	38.3653	0.4523	QSO	2590.5359
2025wek	237.0823	32.7603	0.7406	GALAXY	4696.9613
2025vjj	236.3173	29.5315	0.1115	GALAXY	534.7696
2025uvu	236.7140	29.9974	0.1131	GALAXY	542.6445
2025uvt	238.8827	31.0152	0.6878	GALAXY	4291.7750
2025uuc	264.9935	53.3381	2.6640	QSO	22,550.7862
2025uua	261.4404	51.9287	0.2819	QSO	1492.0705
2025uxo	248.8887	41.0160	0.1327	GALAXY	645.0393
2025uvs	269.2136	55.3507	0.1918	GALAXY	966.3277
2025utz	247.7828	40.7122	0.2576	GALAXY	1346.3430
2025usn	237.6129	30.3335	0.2167	GALAXY	1107.2874
2025vyh	272.3377	59.0274	1.2842	GALAXY	9243.8722
2025vqh	270.4048	59.0388	0.1501	GALAXY	737.4811
2025vpk	43.2179	−11.1208	0.1109	GALAXY	531.5151
2025vki	289.0243	61.5418	0.1703	QSO	846.8556
2025vad	237.2357	28.6868	0.2982	QSO	1591.4464
2025vax	241.0787	32.3593	0.3191	GALAXY	1720.6413
2025vau	234.3892	29.6584	0.5778	GALAXY	3474.1519
2025vat	233.0135	27.5936	0.8388	GALAXY	5471.1382
2025uog	58.3271	−33.1842	0.3482	GALAXY	1904.6131
2025unn	239.1649	33.2565	0.3183	GALAXY	1715.6246
2025unm	247.0437	42.0718	0.3651	GALAXY	2012.6763
2025unl	250.1464	46.7457	0.2294	GALAXY	1180.3280
2025wge	242.0833	40.0865	0.1323	GALAXY	642.7407
2025uzn	235.2263	31.3966	0.2921	GALAXY	1553.9217
2025vap	265.4473	52.2285	0.1716	GALAXY	854.4513
2025vae	234.2501	24.4684	0.2061	GALAXY	1046.8841
2025uuk	262.3959	54.6045	0.2089	GALAXY	1062.8393
2025uui	239.7301	30.9933	0.1736	GALAXY	865.0194
2025uuh	283.7587	60.1951	0.1645	GALAXY	815.3669
2025uzg	233.7462	24.8625	0.2292	GALAXY	1179.1234
2025uzf	255.1250	49.6714	0.1688	GALAXY	839.0211
2025unk	246.3895	40.7262	0.4073	GALAXY	2288.6124
2025wku	282.0333	60.8339	0.1943	GALAXY	980.0172
2025utt	267.5892	54.9656	0.2685	QSO	1411.0327
2025uql	267.2358	57.8760	0.1478	GALAXY	725.1096
2025ung	251.2007	44.2291	0.1803	QSO	902.0566

Table 5
(Continued)

TNS Name	R.A. Host	Decl. Host	z	Spectype	D_L [Mpc]
2025wnj	257.3367	54.1327	0.1663	GALAXY	825.3396
2025wmh	43.5906	-6.5685	0.1402	GALAXY	684.6676
2025wiq	35.6168	3.1288	0.2159	GALAXY	1102.4901
2025vak	237.6181	38.5757	0.5645	QSO	3377.9328
2025vah	239.4819	29.2198	1.2998	GALAXY	9382.7814
2025uzt	236.2475	35.7668	0.2820	GALAXY	1492.4074
2025uph	297.0632	64.6738	0.1814	GALAXY	908.4743
2025unr	220.8747	13.1996	0.1189	GALAXY	572.5861
2025vtg	37.8268	-0.1797	0.2751	GALAXY	1450.6962
2025vmd	39.4021	-9.5487	0.1580	GALAXY	780.1118
2025wcz	35.7978	1.9576	0.2057	GALAXY	1044.5975
2025vvs	37.6256	-0.6878	0.2932	GALAXY	1560.6515
2025vun	37.6251	3.0939	0.2454	GALAXY	1274.0367
2025wew	36.9475	1.1849	1.9112	QSO	15,065.3336
2025wdi	35.0614	1.9105	0.1234	GALAXY	595.9829

Appendix D
Targeted Follow-up of DESI Candidate Host Galaxies

Here we list the DESI-selected candidate hosts followed up with 3KK/FTW (Table 6). The target selection was based on a combination of the individual 3D probability (P3D) (similar to L. P. Singer et al. 2016) of each galaxy w.r.t. the GW localization as well as the luminosity L_r in the r band as a proxy for stellar mass. Potential targets were drawn from a daily updated DESI catalog with application of common quality cuts. At the time of the observations, only the `bayestar.multiorder.fits,1` map was available. The product (P3D$\cdot L_r$) is unitless after being normalized to sum to one in the limit where galaxies follow a Schechter luminosity function ($\Phi_* = 1.0 \cdot 10^{-9}\ h^{-3}\ \mathrm{Mpc}^{-3}\mathrm{dex}^{-1}$, $M_* - 5\log(h) = 21.0$, $\alpha = 1.27$) and are randomly distributed in 3D. Therefore, this quantity represents an estimate of the probability that each target is the true host. The total probability covered by these 10 galaxies sums to ≈1%. A KN-like transient would have been confidently detected in the r band for all targets when comparing with AT2025gfo. In the i band and J band, only S250818k_162333_p390716, S250818k_161052_p415309, and S250818k_160742_p385551 would have been detected. The absolute magnitudes of the other targets in these bands were slightly fainter than the reference values from AT2025gfo. The absolute magnitude reference values of AT2025gfo, taken 1.927, 1.863, and 2.170 days postmerger in the r, i, and J bands, are −14.55, −14.83 (I. Andreoni et al. 2017), and −15.32 (Y. Utsumi et al. 2017; V. A. Villar et al. 2017).

Table 6
List of Potential Host Galaxies Identified by Their 3D Localization including DESI Redshifts Followed Up with Targeted 3KK/FTW Observations, Based on the Full `bayestar.multiorder.fits,1` Map

Internal Name	R.A. (deg)	Decl. (deg)	z	D_L (Mpc)	P3D$\cdot L_r$	$t_{\mathrm{obs}} - t_0$ (days)	M_r^{lim}	M_i^{lim}	M_J^{lim}
S250818k_160742_p385551	241.9235	38.9307	0.03851	175.6	0.00103	1.8324	−12.76	−14.02	−15.05
S250818k_162333_p390716	245.8864	39.1211	0.03503	159.3	0.00100	1.8398	−12.70	−13.97	−15.24
S250818k_160011_p400610	240.0455	40.1027	0.06199	287.4	0.00071	1.8472	−13.95	−15.18	−15.56
S250818k_155915_p400626	239.8124	40.1073	0.07070	329.8	0.00067	1.8547	−14.33	−15.56	−15.91
S250818k_161800_p412332	244.5018	41.3922	0.06120	283.6	0.00072	1.8621	−13.86	−15.12	−15.39
S250818k_161052_p415309	242.7175	41.8858	0.03826	174.4	0.00084	1.8695	−12.90	−14.14	−14.46
S250818k_161833_p430453	244.6389	43.0814	0.05992	277.4	0.00200	1.8769	−13.88	−15.13	−15.49
S250818k_161505_p433544	243.7694	43.5955	0.06516	302.8	0.00155	1.8843	−14.11	−15.45	−15.79
S250818k_162631_p435826	246.6295	43.9740	0.05917	273.8	0.00081	1.8917	−13.89	−15.22	−15.57
S250818k_170818_p452118	257.0755	45.3551	0.06057	280.6	0.00077	1.8992	−13.87	−15.26	−15.59

Notes. No transients were seen in difference imaging. The table includes the internal name, R.A. and decl. in degrees, host redshift z, luminosity distance D_L, normalized true host probability P3D$\cdot L_r$, time difference between the GW signal t_0 and start of observations t_{obs}, and individual 3σ absolute magnitude limit in the respective bands $M_{r/i/J}^{\mathrm{lim}}$.

ORCID iDs

Xander J. Hall https://orcid.org/0000-0002-9364-5419
Antonella Palmese https://orcid.org/0000-0002-6011-0530
Brendan O'Connor https://orcid.org/0000-0002-9700-0036
Daniel Gruen https://orcid.org/0000-0003-3270-7644
Malte Busmann https://orcid.org/0009-0001-0574-2332
Julius Gassert https://orcid.org/0009-0008-2754-1946
Lei Hu https://orcid.org/0000-0001-7201-1938
Ignacio Magaña Hernandez https://orcid.org/0000-0003-2362-0459
Jessica Nicole Aguilar https://orcid.org/0000-0003-0822-452X
Ariel Amsellem https://orcid.org/0000-0003-3433-2698
Steven Ahlen https://orcid.org/0000-0001-6098-7247
John Banovetz https://orcid.org/0000-0003-0776-8859
Segev BenZvi https://orcid.org/0000-0001-5537-4710
Davide Bianchi https://orcid.org/0000-0001-9712-0006
David Brooks https://orcid.org/0000-0002-8458-5047
Francisco Javier Castander https://orcid.org/0000-0001-7316-4573
Andrei Cuceu https://orcid.org/0000-0002-2169-0595
Arjun Dey https://orcid.org/0000-0002-4928-4003
Peter Doel https://orcid.org/0000-0002-6397-4457
Jennifer Fabà-Moreno https://orcid.org/0009-0006-7670-9843
Simone Ferraro https://orcid.org/0000-0003-4992-7854
Andreu Font-Ribera https://orcid.org/0000-0002-3033-7312
Jaime E. Forero-Romero https://orcid.org/0000-0002-2890-3725
Gaston Gutierrez https://orcid.org/0000-0003-0825-0517
Laurent Le Guillou https://orcid.org/0000-0001-7178-8868
Dick Joyce https://orcid.org/0000-0003-0201-5241
Theodore Kisner https://orcid.org/0000-0003-3510-7134
Anthony Kremin https://orcid.org/0000-0001-6356-7424
Claire Lamman https://orcid.org/0000-0002-6731-9329
Martin Landriau https://orcid.org/0000-0003-1838-8528
Michael Levi https://orcid.org/0000-0003-1887-1018
Axel de la Macorra https://orcid.org/0000-0002-1769-1640
Marc Manera https://orcid.org/0000-0003-4962-8934
Aaron Meisner https://orcid.org/0000-0002-1125-7384
Ramon Miquel https://orcid.org/0000-0002-6610-4836
John Moustakas https://orcid.org/0000-0002-2733-4559
Seshadri Nadathur https://orcid.org/0000-0001-9070-3102
Francisco Prada https://orcid.org/0000-0001-7145-8674
Ignasi Pérez-Ràfols https://orcid.org/0000-0001-6979-0125
Eusebio Sanchez https://orcid.org/0000-0002-9646-8198
David Schlegel https://orcid.org/0000-0002-5042-5088
David Sprayberry https://orcid.org/0000-0001-7583-6441
Gregory Tarlé https://orcid.org/0000-0003-1704-0781
Rongpu Zhou https://orcid.org/0000-0001-5381-4372
Hu Zou https://orcid.org/0000-0002-6684-3997

References

Abbott, B. P., Abbott, R., Abbott, T. D., et al. 2017, PhRvL, 119, 161101
Abbott, R., Abbott, T. D., Acernese, F., et al. 2023, PhRvX, 13, 011048
Aghanim, N., Akrami, Y., Ashdown, M., et al. 2020, A&A, 641, A6
Ahumada, R., Allende Prieto, C., Almeida, A., et al. 2020, ApJS, 249, 3
Amsellem, A. J., Palmese, A., Douglass, K., et al. 2025, arXiv:2512.08818
Andreoni, I., Ackley, K., Cooke, J., et al. 2017, PASA, 34, e069
Arcavi, I., Hosseinzadeh, G., Howell, D. A., et al. 2017, Natur, 551, 64
Ashton, G., Ackley, K., Hernandez, I. M., & Piotrzkowski, B. 2021, CQGra, 38, 235004
Ashton, G., Burns, E., Canton, T. D., et al. 2018, ApJ, 860, 6
Ashton, G., Hübner, M., Lasky, P. D., et al. 2019, ApJS, 241, 27
Baldwin, J. A., Phillips, M. M., & Terlevich, R. 1981, PASP, 93, 5
Ballard, W., Palmese, A., Hernandez, I. M., et al. 2023, RNAAS, 7, 250
Banerjee, S., Botticella, M., Brennan, S. J., et al. 2025a, TNSCR 2025-3373
Banerjee, S., Botticella, M.-T., Brennan, S. J., et al. 2025b, GCN, 41532, 1
Becerra, R. L., Yang, Y., Watson, A. M., Troja, E., & Lee, W. H. 2025, GCN, 41544, 1
Beck, R., Dobos, L., Budavári, T., Szalay, A. S., & Csabai, I. 2016, MNRAS, 460, 1371
Berger, E., Fong, W., & Chornock, R. 2013, ApJL, 774, L23
Bhardwaj, M., Palmese, A., Magaña Hernandez, I., D'Emilio, V., & Morisaki, S. 2024, ApJ, 977, 122
Bianchi, L., Shiao, B., & Thilker, D. 2017, ApJS, 230, 24
Bruni, G., Piro, L., Gianfagna, G., & Thakur, A. L. 2025, GCN, 41500, 1
Busmann, M., Hall, X. J., Gruen, D., O'Connor, B., & Palmese, A. 2025a, GCN, 41421, 1
Busmann, M., O'Connor, B., Sommer, J., et al. 2025b, A&A, 701, A225
Calzetti, D. 2013, in Secular Evolution of Galaxies, ed. J. Falcón-Barroso & J. H. Knapen, 419 (Cambridge Univ. Press)
Calzetti, D., Kinney, A. L., & Storchi-Bergmann, T. 1994, ApJ, 429, 582
Chabrier, G. 2003, PASP, 115, 763
Chambers, K. C., Boer, T. D., Fairlamb, J., et al. 2025a, TNSTR 2025-3320,
Chambers, K. C., Boer, T. D., Fairlamb, J., et al. 2025b, TNSTR 2025-3320,
Chambers, K. C., Magnier, E. A., Metcalfe, N., et al. 2016, arXiv:1612.05560
Chen, Y.-X., & Metzger, B. D. 2025, ApJL, 991, L22
Condon, J. J. 1992, ARA&A, 30, 575
Coulter, D. A., Foley, R. J., Kilpatrick, C. D., et al. 2017, Sci, 358, 1556
DESI Collaboration, Abareshi, B., Aguilar, J., et al. 2022, AJ, 164, 207
DESI Collaboration, Abdul-Karim, M., Adame, A. G., et al. 2025a, arXiv:2503.14745
DESI Collaboration, Abdul-Karim, M., Aguilar, J., et al. 2025b, arXiv:2503.14738v2
DESI Collaboration, Aghamousa, A., Aguilar, J., et al. 2016, arXiv:1611.00037
Dey, A., Schlegel, D. J., Lang, D., et al. 2019, AJ, 157, 168
Draine, B. T., & Li, A. 2007, ApJ, 657, 810
Drout, M. R., Piro, A. L., Shappee, B. J., et al. 2017, Sci, 358, 1570
Evans, P. A., Cenko, S. B., Kennea, J. A., et al. 2017, Sci, 358, 1565
Fitzpatrick, E. L. 1999, PASP, 111, 63
Fong, W., Laskar, T., Rastinejad, J., et al. 2021, ApJ, 906, 127
Fong, W.-f., Nugent, A. E., Dong, Y., et al. 2022, ApJ, 940, 56
Franz, N., Subrayan, B., Kilpatrick, C. D., et al. 2025, ApJ, 994, L45
Freeburn, J., O'Connor, B., Hall, X. J., et al. 2025, GCN, 41507, 1
Fremling, C., Neill, D., & Sharma, Y. 2025, TNSCR 2025-3508,
Gaia Collaboration, Brown, A. G. A., Vallenari, A., et al. 2021, A&A, 649, A1
Gal-Yam, A., Fox, D. B., Price, P. A., et al. 2006, Natur, 444, 1053
Gehrels, N., Cannizzo, J. K., Kanner, J., et al. 2016, ApJ, 820, 136
Gillanders, J. H., Huber, M. E., Chambers, K. C., et al. 2025a, GCN, 41540, 1
Gillanders, J. H., Huber, M. E., Nicholl, M., et al. 2025b, arXiv:2510.01142
Goldstein, A., Veres, P., Burns, E., et al. 2017, ApJL, 848, L14
Goldwasser, S., Yaron, O., Sass, A., et al. 2022, TNSAN 191,
Gössl, C. A., & Riffeser, A. 2002, A&A, 381, 1095
Guy, J., Bailey, S., Kremin, A., et al. 2023, AJ, 165, 144
Hahn, C., Wilson, M. J., Ruiz-Macias, O., et al. 2023, AJ, 165, 253
Hall, X. J., Busmann, M., Gruen, D., O'Connor, B., & Palmese, A. 2025a, GCN, 41433, 1
Hall, X. J., Busmann, M., Koehn, H., et al. 2025b, arXiv:2510.24620
Hall, X. J., Hu, L., Palmese, A., et al. 2025c, TNSAN 84,
Hall, X. J., Palmese, A., BenZvi, S., et al. 2026, arXiv:2601.12611
Hopp, U., Bender, R., Grupp, F., et al. 2014, SPIE, 9145, 91452D
Jin, Z.-P., Hotokezaka, K., Li, X., et al. 2016, NatCo, 7, 12898
Johnson, B. D., Leja, J., Conroy, C., & Speagle, J. S. 2021, ApJS, 254, 22
Johnson, B. D., Leja, J. L., Conroy, C., & Speagle, J. S. 2019, Prospector: Stellar population inference from spectra and SEDs, v1.4.0, Astrophysics Source Code Library, ascl:1905.025
Jones, D. O., French, K. D., Agnello, A., et al. 2025, TNSTR 2025-3279,
Kaiser, N., Burgett, W., Chambers, K., et al. 2010, SPIE, 7733, 77330E
Kasliwal, M. M., Ahumada, T., Stein, R., et al. 2025, ApJ, 995, L59
Kauffmann, G., Heckman, T. M., Tremonti, C., et al. 2003, MNRAS, 346, 1055
Kaur, R., O'Connor, B., Palmese, A., & Kunnumkai, K. 2026, ApJ, 1000, 74
Kennicutt, R. C., & Evans, N. J. 2012, ARA&A, 50, 531

Kewley, L. J., Dopita, M. A., Sutherland, R. S., Heisler, C. A., & Trevena, J. 2001, ApJ, 556, 121
Kewley, L. J., Groves, B., Kauffmann, G., & Heckman, T. 2006, MNRAS, 372, 961
Kron, R. G. 1980, ApJS, 43, 305
Kunnumkai, K., Palmese, A., Bulla, M., et al. 2025a, PhRvD, 112, 123005
Kunnumkai, K., Palmese, A., Farah, A. M., et al. 2025b, ApJ, 993, 15
Lang-Bardl, F., Bender, R., Goessl, C., et al. 2016, SPIE, 9908, 990844
Leja, J., Johnson, B. D., Conroy, C., van Dokkum, P. G., & Byler, N. 2017, ApJ, 837, 170
Lerner, Y., Stone, N. C., & Ofengeim, D. D. 2026, MNRAS, 545, staf1835
Levan, A., Gompertz, B. P., Salafia, O. S., et al. 2024, Natur, 626, 737
The LIGO Scientific Collaborationthe Virgo Collaborationthe KAGRA Collaboration, et al. 2025, arXiv:2508.18083
Ligo Scientific CollaborationVIRGO CollaborationKagra Collaboration 2025, GCN, 41437, 1
Magaña Hernandez, I., D'Emilio, V., Morisaki, S., Bhardwaj, M., & Palmese, A. 2024, ApJL, 971, L5
Masci, F. J., Laher, R. R., Rusholme, B., et al. 2023, arXiv:2305.16279
Metzger, B. D., Hui, L., & Cantiello, M. 2024, ApJL, 971, L34
Miller, T. N., Doel, P., Gutierrez, G., et al. 2024, AJ, 168, 95
Moustakas, J., Scholte, D., Dey, B., & Khederlarian, A. 2023, FastSpecFit: Fast spectral synthesis and emission-line fitting of DESI spectra, Astrophysics Source Code Library, ascl:2308.005 Version:3.2.1
Müller-Bravo, T., & Galbany, L. 2022, JOSS, 7, 4508
Murphy, E. J., Condon, J. J., Schinnerer, E., et al. 2011, ApJ, 737, 67
Nenkova, M., Sirocky, M. M., Ivezić, Ž., & Elitzur, M. 2008, ApJ, 685, 147
Nugent, A. E., Fong, W. F., Dong, Y., et al. 2022, ApJ, 940, 57
O'Connor, B., Ricci, R., Troja, E., et al. 2025, ApJ, 995, L47
O'Connor, B., Troja, E., Dichiara, S., et al. 2021, MNRAS, 502, 1279
O'Connor, B., Troja, E., Dichiara, S., et al. 2022, MNRAS, 515, 4890
Ofek, E. O., Konno, R., Zimmerman, E. A., et al. 2025, TNSTR 2025-3434,
Palmese, A., Bom, C. R., Mucesh, S., & Hartley, W. G. 2023, ApJ, 943, 56
Palmese, A., Graur, O., Annis, J. T., et al. 2019, BAAS, 51, 310
Palmese, A., Hartley, W., Tarsitano, F., et al. 2017, ApJ, 849, L34
Perley, D. A., Kasliwal, M. M., Karambelkar, V., et al. 2025, GCN, 41480, 1
Piotrzkowski, B., Baylor, A., & Hernandez, I. M. 2022, CQGra, 39, 085010
Piro, A. L., & Pfahl, E. 2007, ApJ, 658, 1173
Poppett, C., Tyas, L., Aguilar, J., et al. 2024, AJ, 168, 245
Rastinejad, J. C., Gompertz, B. P., Levan, A. J., et al. 2022, Natur, 612, 223
Riess, A. G., Yuan, W., Macri, L. M., et al. 2022, ApJ, 934, L7
Savchenko, V., Ferrigno, C., Kuulkers, E., et al. 2017, ApJL, 848, L15
Schlafly, E. F., & Finkbeiner, D. P. 2011, ApJ, 737, 103
Schlafly, E. F., Kirkby, D., Schlegel, D. J., et al. 2023, AJ, 166, 259
Schulze, S., Yaron, O., Sollerman, J., et al. 2021, ApJS, 255, 29
Singer, L. P., Chen, H.-Y., Holz, D. E., et al. 2016, ApJL, 829, L15
Skrutskie, M. F., Cutri, R. M., Stiening, R., et al. 2006, AJ, 131, 1163
Smith, M., Sullivan, M., Wiseman, P., et al. 2020, MNRAS, 494, 4426
Soares-Santos, M., Holz, D. E., Annis, J., et al. 2017, ApJL, 848, L16
Sollerman, J., Fremling, C., Perley, D., & Laz, T. D. 2025a, TNSTR 2025-3397,
Sollerman, J., Mehla, A., Chu, M., & Fremling, C. 2025b, TNSCR 2025-3920,
Soumagnac, M. T., Nugent, P., Knop, R. A., et al. 2024, ApJS, 275, 22
Stein, R. 2025, TNSTR 2025-3325,
Stein, R., Ahumada, T., Kasliwal, M., et al. 2025, GCN, 41414, 1
Sullivan, M., Le Borgne, D., Pritchet, C. J., et al. 2006, ApJ, 648, 868
Tanvir, N. R., Levan, A. J., Fruchter, A. S., et al. 2013, Natur, 500, 547
Tonry, J., Denneau, L., Weiland, H., et al. 2025, TNSTR 2025-3286,
Troja, E., Castro-Tirado, A. J., Becerra González, J., et al. 2019, MNRAS, 489, 2104
Troja, E., Fryer, C. L., O'Connor, B., et al. 2022, Natur, 612, 228
Troja, E., Piro, L., van Eerten, H., et al. 2017, Natur, 551, 71
Troja, E., Ryan, G., Piro, L., et al. 2018, NatCo, 9, 4089
Utsumi, Y., Tanaka, M., Tominaga, N., et al. 2017, PASJ, 69, 101
Villar, V. A., Guillochon, J., Berger, E., et al. 2017, ApJL, 851, L21
Wise, J., Covarrubias, S., Chu, M., & Fremling, C. 2025, TNSCR 2025-3869,
Wright, E. L., Eisenhardt, P. R. M., Mainzer, A. K., et al. 2010, AJ, 140, 1868
Yang, Y.-H., Troja, E., O'Connor, B., et al. 2024, Natur, 626, 742
Yang, Y. H., Troja, E., Ristić, M., et al. 2026, ApJ, 996, L24
Zou, H., Gao, J., Zhou, X., & Kong, X. 2019, ApJS, 242, 8